Please cite this article in press as: Harcombe et al., Metabolic Resource Allocation in Individual Microbes Determines Ecosystem Interactions and Spatial Dynamics, Cell Reports (2014), http://dx.doi.org/10.1016/j.celrep.2014.03.070

Cell Reports
Article

Metabolic Resource Allocation in Individual Microbes Determines Ecosystem Interactions and Spatial Dynamics

William R. Harcombe,[1,7,8] William J. Riehl,[2,7,9] Ilija Dukovski,[2] Brian R. Granger,[2] Alex Betts,[1,10] Alex H. Lang,[3] Gracia Bonilla,[2] Amrita Kar,[2] Nicholas Leiby,[1,4] Pankaj Mehta,[2,3] Christopher J. Marx,[1,5,11,*] and Daniel Segrè[2,6,*]
[1]Department of Organismic and Evolutionary Biology, Harvard University, Cambridge, MA 02138, USA
[2]Bioinformatics Graduate Program, Boston University, Boston, MA 02215, USA
[3]Department of Physics, Boston University, Boston, MA 02215, USA
[4]Systems Biology Graduate Program, Harvard University, Cambridge, MA 02138, USA
[5]Faculty of Arts and Sciences Center for Systems Biology, Harvard University, Cambridge, MA 02138, USA
[6]Department of Biology and Department of Biomedical Engineering, Boston University, Boston, MA 02215, USA
[7]Co-first author
[8]Present address: Department of Ecology, Evolution, and Behavior, University of Minnesota, St. Paul, MN 55108, USA
[9]Present address: Lawrence Berkeley National Laboratory, Berkeley, CA 94720, USA
[10]Present address: Department of Zoology, University of Oxford, Oxford OX1 3PS, UK
[11]Present address: Department of Biological Sciences, University of Idaho, Moscow, ID 83844, USA
*Correspondence: cmarx@uidaho.edu (C.J.M.), dsegre@bu.edu (D.S.)
http://dx.doi.org/10.1016/j.celrep.2014.03.070

SUMMARY

The interspecies exchange of metabolites plays a key role in the spatiotemporal dynamics of microbial communities. This raises the question of whether ecosystem-level behavior of structured communities can be predicted using genome-scale metabolic models for multiple organisms. We developed a modeling framework that integrates dynamic flux balance analysis with diffusion on a lattice and applied it to engineered communities. First, we predicted and experimentally confirmed the species ratio to which a two-species mutualistic consortium converges and the equilibrium composition of a newly engineered three-member community. We next identified a specific spatial arrangement of colonies, which gives rise to what we term the "eclipse dilemma": does a competitor placed between a colony and its cross-feeding partner benefit or hurt growth of the original colony? Our experimentally validated finding that the net outcome is beneficial highlights the complex nature of metabolic interactions in microbial communities while at the same time demonstrating their predictability.

INTRODUCTION

Although often studied alone in well-mixed flasks, most microbial organisms live in multispecies, structured, and highly dynamic consortia (Denef et al., 2010; Dethlefsen et al., 2007; Lozupone et al., 2012; Ramette and Tiedje, 2007; Xavier and Foster, 2007). Interactions of microbes with each other and with the environment play a fundamental role in the evolution and dynamics of these communities. Many of these interactions are mediated by the uptake and excretion of small molecules, produced and degraded by the metabolic network encoded within each organism. In turn, the ensuing spatiotemporal changes of nutrients and by-products in the environment continually modify the conditions sensed by individual cells, causing transient niches and context-dependent interspecies interactions.

Given this complexity, one may ask whether a suitable mathematical modeling framework could help bridge the gap between metabolic strategies of individual species and ecosystem-level dynamics. Such a framework would be a powerful instrument for microbial ecology, with potential impact on research areas as diverse as biogeochemical cycles (Falkowski et al., 2008), the health-balancing role of the human microbiome (Lozupone et al., 2012; Turnbaugh et al., 2007), and synthetic ecology (Klitgord and Segrè, 2011; Park et al., 2011; Shou et al., 2007). Moreover, fundamental questions on the stability (May, 1973; Mougi and Kondoh, 2012) and diversity (Curtis et al., 2002; Gudelj et al., 2010) of microbial ecosystems, the evolution of cooperation (Harcombe, 2010; Xavier and Foster, 2007), and the emergence of multicellularity (Pfeiffer and Bonhoeffer, 2003) lie precisely at the boundary between the metabolic requirements of individual species and the community-level implications of shared resources.

The past decade has seen the emergence of several novel experimental systems for investigating the dynamics of structured microbial consortia. For example, spatial structure was shown to be critical for maintaining diversity in systems with antagonistic interactions, ranging from chemical warfare (Kerr et al., 2002) to predator-prey behavior (Balagaddé et al., 2008), as well as beneficial interactions (Kim et al., 2008). In terms of metabolism, a variety of novel, engineered mutualisms between

Please cite this article in press as: Harcombe et al., Metabolic Resource Allocation in Individual Microbes Determines Ecosystem Interactions and Spatial Dynamics, Cell Reports (2014), http://dx.doi.org/10.1016/j.celrep.2014.03.070

codependent strains have been developed (Harcombe, 2010; Hillesland and Stahl, 2010; Shou et al., 2007). These include a laboratory-evolved costly cooperation between *Salmonella enterica* serovar *typhimurium* LT2 and an auxotrophic *Escherichia coli* K12 strain (Harcombe, 2010), which we use as a starting point in the current work.

Although some qualitative results, such as the importance of spatial structure in a two-species system, are consistent with theory on the evolution of cooperation (Sachs et al., 2004), broader and more quantitative predictions such as species ratios or interactions between a larger number of players are unexplored experimentally and computationally. How predictable are consortia compositions in spatially structured environments, and how strongly are they affected by initial species frequencies? Can stable systems be engineered with more than two species? Can interspecies interactions in synthetic microbial consortia emerge as a consequence of individual species solving their own metabolic resource allocation problem?

From a theoretical perspective, these questions bridge multiple distinct scales, from individual intracellular reactions, up to the spatial distributions of multiple species and environmental metabolites (Gudelj et al., 2010; MacLean and Gudelj, 2006). Classical ordinary differential equation (ODE) models have been shown to recapitulate colony diameter and height as a function of time (Kamath and Bungay, 1988; Pipe and Grimson, 2008; Pirt, 1967; Rieck et al., 1973). Agent-based models have successfully shown how colony morphology arises as an emergent property of the behavior of individual cells or clusters of cells (Ben-Jacob et al., 1998; Kreft et al., 1998, 2001; Xavier et al., 2005). However, these approaches typically assume simple interspecies interaction rules rather than computing them based on detailed representations of intracellular biochemical networks.

In contrast, stoichiometric modeling, a class of systems biology methods with roots in metabolic engineering, has been shown to provide testable predictions of metabolic activity at the whole genome scale, with no need for the hundreds of differential equations and kinetic parameters typical of classical kinetic models. One of the most broadly used methods, flux balance analysis (FBA) (Orth et al., 2010) assumes steady state and optimality to predict metabolic rates (fluxes) of all reactions in the cell, including uptake and secretion fluxes, and the amount of microbial growth (Harcombe et al., 2013; McCloskey et al., 2013; Segrè et al., 2002). It is important to keep in mind that the simplifications that make FBA efficient and useful are also among the main reasons for its limitations, including the incapacity to predict intracellular metabolite concentrations, the reliance on a predefined metabolic objective, and the need for prior knowledge of biomass composition. Alternative uses of stoichiometric constrains (e.g., sampling of the feasible space [Bordel et al., 2010]), integration with high-throughput data (Becker and Palsson, 2008; Collins et al., 2012), and thermodynamics or economy-inspired theory (Fleming et al., 2012; De Martino et al., 2012; Reznik et al., 2013; Schuetz et al., 2012) are among the new directions being sought in order to overcome some of these limitations.

Recent efforts have shown how FBA can be extended to model metabolite-mediated interactions between different species in microbial consortia (Klitgord and Segrè, 2011), e.g., by searching for syntrophic compositions (Stolyar et al., 2007), interaction-inducing environments (Klitgord and Segrè, 2010), competition/cooperation balances (Freilich et al., 2011; Wintermute and Silver, 2010), or multilevel optima (Zomorrodi and Maranas, 2012) in multispecies joint stoichiometric models, or by implementing dynamic flux balance modeling of cocultures (Khandelwal et al., 2013; Salimi et al., 2010). Some of these approaches require a priori assumptions on how two species interact, e.g., a tunable ratio of the biomass production rates (Stolyar et al., 2007), a minimal growth rate for each species (Klitgord and Segrè, 2010), or different types of joint or multilevel objective functions (Freilich et al., 2011; Wintermute and Silver, 2010; Zomorrodi and Maranas, 2012). Most importantly, to our knowledge, these approaches have not been extended to multispecies communities in a structured environment, although a single-species model has been previously coupled with reactive transport (Scheibe et al., 2009).

Here, we introduce a multiscale modeling framework that computes ecosystem-level spatiotemporal dynamics based on detailed intracellular metabolic stoichiometry, without any a priori assumption on whether and how different species would interact. Our approach, named Computation of Microbial Ecosystems in Time and Space (COMETS), implements a dynamic FBA algorithm on a lattice, making it possible to track the spatiotemporal dynamics of multiple microbial species in complex environments with complete genome scale resolution. We apply COMETS to the study of a previously built *E. coli*/*S. enterica* synthetic consortium (Harcombe, 2010) and to a new three-member consortium that incorporates *Methylobacterium extorquens* AM1 into the *E. coli*/*S. enterica* system.

RESULTS

From Genome Scale to Ecosystem-Level Spatiotemporal Models

COMETS uses dynamic flux balance analysis (dFBA) (Mahadevan et al., 2002) to perform time-dependent metabolic simulations of microbial ecosystems, bridging the gap between stoichiometric and environmental modeling. Simulations occur on a spatially structured lattice of interacting metabolic subsystems (“boxes”), providing at the same time insight on intracellular metabolic fluxes and on ecosystem-level distributions of microbial populations and nutrients. COMETS incorporates two fundamental steps (Figure 1; Experimental Procedures). The first step, cellular growth, is modeled as an increase of biomass at different spatial locations, using a hybrid kinetic-dFBA algorithm. Each box may contain biomass for an arbitrary number of different species. The second step consists of a finite differences approximation of the diffusion of extracellular nutrients and by-products in the environment, and of the expansion of biomass (see Experimental Procedures). Simple diffusion simulations in absence of growth behave as expected (Figure S1, related to Figure 1). We have incorporated multiple species into COMETS by importing the corresponding stoichiometric models, either from manually curated reconstructions, or from automated pipelines that construct models from annotated genomes and high-throughput data, such as Model SEED (Henry

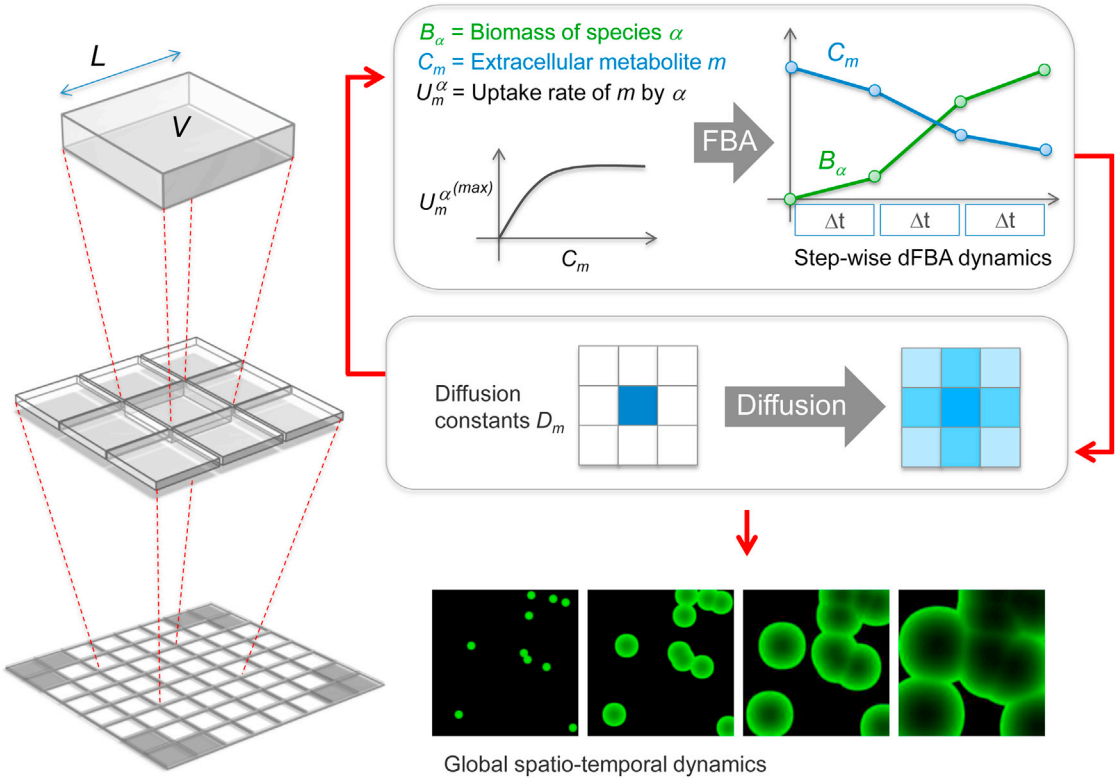

Figure 1. A Schematic Representation of the Key Steps of COMETS Simulations

Schematic representation of the key steps of COMETS simulations from the level of individual boxes (top) to a whole lattice (bottom). Within each box, dFBA is solved for each species, with uptake set by Michaelis-Menten equations (top right). These calculations amount to piecewise linear approximations of the growth and environmental metabolites as a function of time. Classical discretization of the diffusion equation gives local rules for updating biomass and nutrients in each box (middle). The ensuing algorithm computes ecosystem dynamics (bottom) as a function of intracellular metabolism of individual species.

et al., 2010). In addition, both spatially and molecularly complex environments can be designed by the user through an interactive toolbox (Figure S2, related to Figure 1) and simulation outcomes can be analyzed through a visualization tool (Figure S3, related to Figures 1 and 4).

COMETS Recapitulates *E. coli* Colony Growth on Different Substrates

A key step toward modeling growth of spatially structured communities is to make sure that the basic dynamics of colony growth can be well captured by our computational approach, with parameter values estimated from the literature (Table 1). As in any FBA model, COMETS does not require intracellular kinetic parameters. However, in analogy with previous dFBA formulations, COMETS estimates the upper bounds to metabolite uptake rates using a saturation curve, described through standard kinetic parameters V_{max} and K_M. In the simulations presented below, we assumed these parameters to be the same for all metabolites. Substrate-specific values can be easily introduced if known (see Experimental Procedures), though theoretical considerations based on the diffusion-limited nature of uptake kinetics suggest limited substrate-to-substrate variation (Berg and Purcell, 1977). The effects of variations of either universal or substrate-specific uptake kinetics parameters are illustrated in Figure S4 (related to Figures 1 and 2), along with sensitivity to all free parameters in COMETS. Moreover, we show that COMETS simulations are invariant relative to small rescaling of the space and time units (Figure S5, related to Figures 1 and 2).

As a first benchmark for COMETS, we tested its capacity to reproduce the observation that colonies increase linearly in diameter over time (Cooper et al., 1968; Palumbo et al., 1971; Pirt, 1967; Wimpenny, 1979). Simulated colonies of *E. coli* followed this growth pattern with only small deviations from linearity as result of lattice discreteness (Figure 2A). Importantly, COMETS accurately predicted the rate of diameter increase on a variety of carbon sources (Figure 2B) as compared to previously published data by Lewis and Wimpenny (1981). These simulations with different carbon sources required only changes in the initial environmental conditions, with no need for parameter tuning.

Species Ratio Convergence in a Codependent Two-Species Consortium

We next tested the ability of COMETS to predict interactions between members of the *E. coli*/*S. enterica* synthetic consortium mentioned above (Harcombe, 2010). In lactose medium, *Salmonella enterica* Serovar *typhimurium* LT2 relies on carbon

Table 1. COMETS Parameters

Parameter	Value	Reference
Uptake V_{max}	10 mmol/g/hr	Gosset, 2005
Uptake K_m	10 μM	Gosset, 2005
Death rate	1%	Saint-Ruf et al., 2004
Metabolite diffusion	5×10^{-6} cm^2/s	Stewart, 2003
Biomass diffusion	3×10^{-9} cm^2/s[a]	Korolev et al., 2011
Max. colony height	200 μm	Lewis and Wimpenny, 1981
Oxygen concentration	250 $\mu mol/cm^2$	Peters et al., 1987

Like any stoichiometric model, COMETS does not require kinetic parameters for intracellular reactions. However, it does require a few parameters associated with the processes of diffusion, nutrient uptake, and carrying capacity of individual boxes. We set all these basic parameters based on values found in the literature.

[a]The *E. coli* colony growth simulations were run with a biomass diffusion of 3×10^{-10} cm^2/s because the laboratory experiments carried out by Lewis and Wimpenny (1981) used plates made with 1.5% agar rather than the 0.8% agarose used in all other experiments.

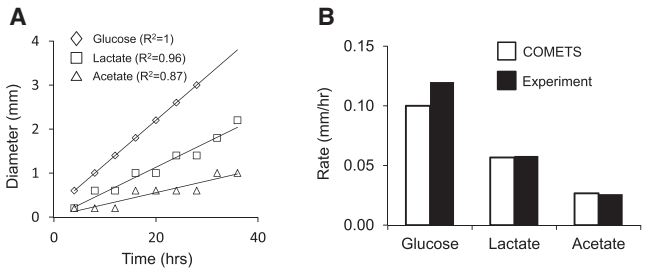

Figure 2. COMETS Predictions of *E. coli* Colony Growth on Various Carbon Sources

(A) COMETS predicts that colony diameter increases linearly on glucose (diamonds), lactate (squares), and acetate (triangles).

(B) COMETS predictions of the rate of colony expansion (white bars) compared to the values reported by Wimpenny (black bars, no error estimate available). Predicted colony expansion on glucose was 16.7% slower than observed, whereas predicted growth on lactate and acetate deviated by 2.7% and 2.2% respectively.

by-products from an *Escherichia coli* K12 *metB* mutant. Reciprocally, this auxotrophic *E. coli* requires methionine from its partner in order to grow in minimal medium. Stoichiometric models of each partner were modified to incorporate known genetic constraints (Figure 3A). For the *E. coli* strain, the *metB* mutation was incorporated by constraining to zero the flux through the corresponding reaction (cystathionine γ-synthase). In *S. enterica*, methionine excretion requires gain-of-function mutations in *metA* (homoserine transsuccinylase) (S.M. Douglas, W.R.H., C.J.M., unpublished data). This excretion was modeled as coupled to biomass, so that as cells grew they excreted observed levels of the amino acid. These genetic alterations created an obligate mutualistic interaction in silico consistent with that observed in the laboratory; neither species was able to grow in isolation on lactose minimal media, but growth was observed when both species were present (Figure 3B).

In order to assess whether COMETS could quantitatively capture community level behavior, we tested its ability to predict the impact of starting conditions on species ratio in our two-species consortium grown on solid medium (Figure 3C). COMETS predicted that, following a single 48 hr growth cycle, communities would converge in composition even when initial frequencies differed by two orders of magnitude (1%–99% *E. coli*). This convergence was indeed observed experimentally over 48 hr, in agreement with previous observations in other model ecosystems (Estrela and Brown, 2013; Shou et al., 2007). More surprisingly, COMETS also correctly predicted the species ratio to which the communities converged in the laboratory. COMETS predicted a composition of 79% ± 4% *E. coli*, which is not significantly different than the experimentally observed frequency of 78% ± 6% (mean ± SD, $p = 0.67$ with a two-tailed t test). As illustrated, for example, in Kerner et al. (2012), predicting species stability and convergence to specific ratios based on simple kinetic models is not a trivial challenge. Furthermore, previous implementations of constraint-based metabolic modeling have struggled to predict which pairs of *E. coli* mutants would coexist, let alone their equilibrium ratios (Wintermute and Silver, 2010).

An Engineered Three-Species Consortium Converges to a Stable Composition

As described above, one of the strengths of COMETS is its ability to handle arbitrarily complex ecosystems. We therefore challenged COMETS to predict the behavior of a tripartite obligate mutualism. Toward this goal, we experimentally engineered a synthetic consortium that incorporates *M. extorquens* AM1 into the previous *E. coli*/*S. enterica* system. This represents a significant advance in complexity relative to obligate consortia that have been previously engineered (Harcombe, 2010; Shou et al., 2007). *M. extorquens* is the best-studied model system for C_1 metabolism (Chistoserdova et al., 2009; Vuilleumier et al., 2009) and has the ability to obtain energy, carbon, and nitrogen from methylamine. Here, we used a Δ*hprA* strain (Marx, 2008) that lacks a key enzyme (hydroxypyruvate reductase) for assimilating carbon from methylamine. In media with lactose and methylamine, the Δ*hprA M. extorquens* strain relies on acetate from *E. coli*, while providing the other two species with a source of nitrogen due to dissimilation of methylamine (Figure 4A). We identify a metabolically engineered obligate mutualism between three species (but see Miller et al., 2010 and Kim et al., 2008 for systems that were not metabolically engineered and Hernández-Sánchez et al., 2013 for a nonobligate system).

COMETS again made accurate predictions about the obligate nature of species interactions in the consortium (Figure 4B). Similarly to the *E. coli* mutant, a model of the engineered *M. extorquens* was created by constraining flux through HprA to zero. COMETS correctly predicted that no species—nor species pair—was capable of growth in lactose-methylamine media. Only when all three species were present was sustained growth observed both in the laboratory and in simulations.

Extending the analysis presented above for the two-species system, we investigated the ability of COMETS to predict the stability and steady-state community composition in our three-species mutualism. COMETS predicted that the community would converge to very similar species ratios from different starting conditions (Figure 4C); after five growth cycles each lasting

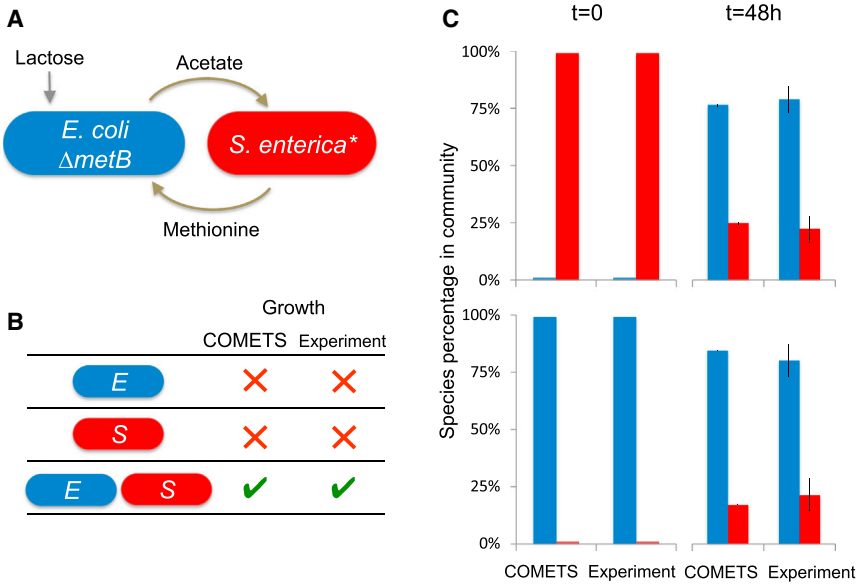

Figure 3. COMETS Predictions of Growth for a Two-Species Synthetic Consortium

(A) The consortium consists of a mutant *S. enterica* that provides methionine to an auxotrophic *E. coli*, obtaining carbon by-products in return.

(B) COMETS correctly predicts that coculture is necessary for growth on lactose minimal medium.

(C) Predicted and observed species frequencies before and after 48 hr of growth. Blue bars correspond to *E. coli*, red bars to *S. enterica*. COMETS ratios (left) represent biomass; observed values (right) are based on cfu.

Error bars are SDs.

96 hr, there was no significant difference between species ratios (*E. coli* p = 0.48, *S. enterica* p = 0.91, *M. extorquens* p = 0.50 with a two-tailed t test). Interestingly, COMETS predicted that *M. extorquens* would dominate the community despite having the lowest maximal growth rate. Experimental observation supported the predicted convergence of community composition over five growth cycles, and the dominance of *M. extorquens* (see also Figure S3, related to Figures 1 and 4).

The Metabolic Eclipse Dilemma: Benefit of a Competitor in Spatially Structured Mutualism

We used the two-species consortium to investigate the influence of spatial structure on competition in mutualistic systems. As a first step, we tested the growth of each partner as a function of increasing distance between them. Consistent with expectations, both the modeled colonies and the observations of the pair exhibited decreased growth as they were initiated further apart (Figure S6, related to Figure 5).

As growth of communities will rarely be as simple as pairwise interactions between microcolonies, we then asked how additional colonies influence pairwise interactions. When essential metabolites diffuse from a point source one might expect that colonies have an "eclipse" effect, casting a resource shadow that reduces the metabolites available to more distant colonies. Based on this logic, one would expect that the growth rate of a colony would be reduced if a competitor colony is placed between the colony and a mutualistic partner (Figure 5A). The extent of negative impact should scale with the rate at which the intermediate colony removes metabolites from the environment. On the other hand, one could argue for an opposite outcome, i.e., that the newly interposed colony, by helping the mutualistic partner, will ultimately benefit the original colony. Intuition alone cannot provide an answer to this conundrum, because its solution depends on the balance among the metabolic rates of the different species, the spatial organization of the colonies, and the diffusion rates.

We used COMETS to simulate the outcome of this gedanken experiment. COMETS predicted that a colony of wild-type *S. enterica* (whose model lacks the imposed methionine excretion of the mutualistic strain) would rapidly remove carbon from its surroundings and diminish the growth of a more distant colony of mutualistic *S. enterica* (Figure 5B). However, if the intermediate colony were another mutualistic *S. enterica*, then, based on COMETS, the growth of the distal colony would end up being larger than in the absence of an interfering colony. Though this effect is predicted to be time dependent, it holds over a substantial temporal window (Figure 5B).

We then tested the computational predictions experimentally and found that after 10 days a colony of *S. enterica* eclipsed by a methionine-excreting competitor produced more biomass than in the absence of a competitor (Figure 5C, p = 0.02 with a two-tailed t test). The intermediate colony increased the growth and excretion of a mutualistic partner, and this amplifying effect outweighed the influence of competition for carbon. In addition to correctly predicting these qualitative behaviors, COMETS also predicted the ratio of distal colony biomasses in the three scenarios (Figure 5C). The difference in the timing at which these ratios were observed (experiment, 240 hr; model, 110 hr) may be partially ascribed to the fact that COMETS does not take into account lag time nor changes in diffusion due to plate drying over this long period.

Thus, based on both the model and the experiment, the metabolic eclipse has the nonintuitive outcome of benefiting the colony that is being eclipsed. Additional insight on the details of this phenomenon would require experimental measurements of metabolite concentrations at different points in space and time, e.g., using imaging mass spectrometry (Louie et al., 2013; Watrous and Dorrestein, 2011). Although this is beyond the scope of the current work, we can use COMETS to provide some preliminary theoretical insight, by taking advantage of its capacity to record simulated fluxes and metabolites at any given time and location for all organisms. This is best illustrated in the heatmaps of Figure 6, which display snapshots of key intracellular transport fluxes (for acetate, methionine, and oxygen), and of the corresponding environmental metabolite concentrations, across different organisms, spatial locations, and time points. The maps provided putative mechanistic insight

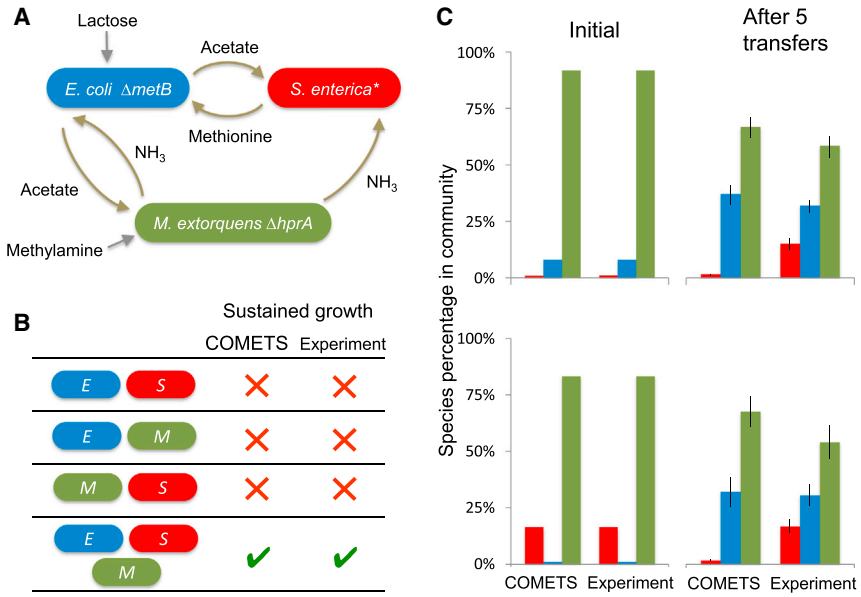

Figure 4. COMETS Predictions of Growth for a Three-Species Consortium

(A) A mutant *M. extorquens* AM1 was added to the two-species system. The *M. extorquens* lacks *hprA*, so it relies on carbon from *E. coli*, while providing the other two species with a source of nitrogen.

(B) COMETS correctly predicts that all three members of the consortium are necessary for growth on lactose/methylamine minimal medium.

(C) Species frequencies before and after five transfers. Blue bars correspond to *E. coli*, red bars to *S. enterica*, and green bars to *M. extorquens*. COMETS ratios (left) represent biomass; observed values (right) are based on cfu. Error bars are SDs.

into how heterogeneity in metabolic phenotypes determined local community composition and function, ultimately driving ecosystem-level dynamics. For example, is it possible to see how acetate uptake/secretion rates diverge over time, matched by methionine fluxes in the opposite directions, and rising levels of oxygen consumption. Helpful insight on the eclipse dilemma can be obtained by further elaboration of the computational data illustrated in Figure 6. In particular, by using the flux values across the different colonies and time points, we were able to determine that the distal *S. enterica* colony took up a lower percentage—but a greater amount—of the acetate excreted by its partner when a competitor was present (Figure 5D).

DISCUSSION

Our results demonstrate that interspecies interactions and microbial community dynamics can emerge as the consequence of individual species locally optimizing intracellular resource allocation. We have used synthetic two- and three-species consortia whose growth depends upon metabolic exchange to experimentally test the predictions of a computational framework that is based entirely on this individual optimality postulate. This approach requires very few free parameters and no a priori assumptions on whether or how species would interact. One notable exception is the need to impose that *S. enterica* secretes methionine as it grows. This requirement, not unlike other flux constraints added in FBA models to match empirical knowledge (such as the maintenance flux), is a consequence of the fact that the specific strain used in the experiment has evolved this secretion capacity as a new trait. Such a trait could not possibly be captured by the standard *S. enterica* FBA model. This current limitation could be addressed by adding in COMETS the capacity for organisms to evolve, i.e., undergo mutations (e.g., in the form of random changes in constraints) and selection (competition between newly emerged variants).

Data from both two- and three-species consortia confirmed predictions that they would repeatedly converge to a steady-state composition even from different starting conditions. The convergence of the two-species consortium is similar to observations with auxotrophic yeast (Shou et al., 2007); our results indicate that this robust behavior extends to the three-species consortium. Here, there was a potential tension between mutualistic interactions and direct competition for limiting nutrients, such as *S. enterica* and *M. extorquens* competing for acetate, and *E. coli* and *S. enterica* competing for ammonia. Particularly surprising was the accuracy of the prediction that the three-species consortium would be dominated by *M. extorquens*—the strain with the slowest maximal growth rate. Whereas the potentially rapid *E. coli* and *S. enterica* faced dual limitations (methionine and N or acetate and N, respectively), *M. extorquens* could access N and energy from methylamine, and the limiting acetate was only required for assimilation. These results are noteworthy in light of the exciting possible opportunities of using synthetic ecology to design microbial consortia for biomedical and metabolic engineering applications. For this goal to come to fruition, it is critical to be able to predict how synthetic communities behave through time, even in heterogeneous environments, such as the lining of a human gut, or the architecture of a leaf. We demonstrated here that the dynamics are repeatable not only within replicates, but between treatments with different starting conditions.

Our experiment on the metabolic eclipse provided a specific, subtle example of COMETS arbitrating between the positive and negative effects that arise from the spatial organization of colonies at a given scale. That proximity of a conspecific competitor could be an advantage due to the stimulation of a shared mutualistic partner highlights the utility and importance of spatially explicit experiments when investigating the nature of interactions in microbial communities. More broadly, the balance between positive and negative effects that arise from local interactions determines changes in community properties such as composition and function and has important implications for the evolutionary dynamics of microbial systems. For example, whether cooperation is selected in structured environments critically depends not only on the qualitative existence of benefits and

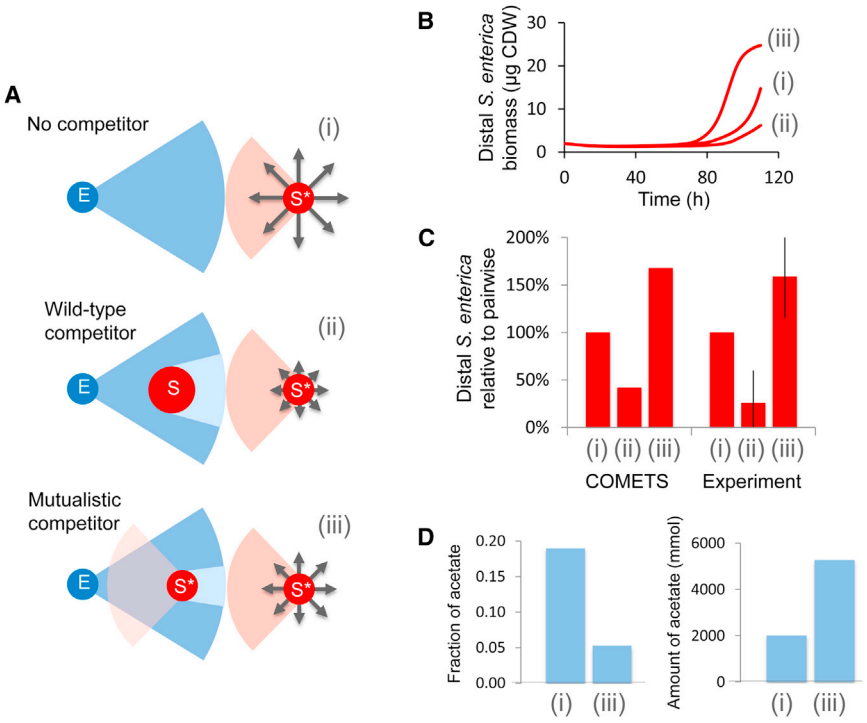

Figure 5. Setup and Results of the Metabolic Eclipse Simulations and Experiments

(A) Setup of the eclipse experiment. The diagram illustrates the positions of the colonies, and the naive expectation that growth of distal *S. enterica* colonies (red circles next to numerals) would be reduced by placement of a competitor between the distal *S. enterica* and its obligate mutualistic partner *E. coli* (blue circles). Relative anticipated growth is represented by gray arrows, methionine diffusing from *S. enterica* colonies is displayed in red, and carbon by-products diffusing from *E. coli* are displayed in blue. Here, S* represents the methionine-excreting *S. enterica*, whereas S represents the wild-type *S. enterica*.

(B) COMETS predicted that wild-type *S. enterica* between *E. coli* and the distal colony would reduce its growth (line (ii)) as compared to the no competitor scenario (line (i)). However, if a second colony of the same methionine-excreting *S. enterica* is placed in the middle, it increases growth of the distal colony (line (iii)).

(C) Growth of the distal colonies standardized to scenario (i) for the case with no competitor (i), wild-type competitor (ii), and mutualistic competitor (iii). COMETS ratios (left three bars) represent biomass; experimental values (right three bars) are based on cfu. Error bars are SDs.

(D) Acetate uptake of distal colonies (i) and (iii) in COMETS. The fraction of acetate is the total uptake of the distal colony divided by the total acetate excretion of its partner. The amount of acetate is the total moles taken up by each colony during the first 89 hr (i.e., before any *E. coli* start to utilize acetate).

costs, but on the quantitative balance between these interactions (Bull and Harcombe, 2009). COMETS has the capacity to evaluate the impact of conflicting types of interactions. For example, the observed dichotomy between fractions and amounts of exchanged nutrients between different species (Figure 5D) may provide a useful starting point for studying the complexity of cross-feeding interactions in natural ecosystems. Moreover, although in this work we focus on interspecies interactions, COMETS can be used to study phenotypic diversity and metabolic heterogeneity within individual colonies. The 3D version of COMETS (under development) will enhance this type of analysis, because it will explicitly account for changes in diffusivity for different molecules (including oxygen) through the colony itself.

The prominent role of optimization in flux balance in general, and in COMETS in particular, deserves further reflection. In COMETS, each organism operates based on its own objective (maximization of biomass, in the current work) given the surrounding nutrient availability. Note that the same species in different spatial locations (in the same in silico experiment) may utilize resources differently (e.g., oxygen-limited biomass in one location will have different physiology than carbon-limited biomass in another). This is an important difference from approaches that optimize the interests of the group and is a central component of COMETS' ability to accurately predict species ratios. However, even the assumption that evolution has acted on a population to optimize a simple objective has been challenged by new data and analyses (Harcombe et al., 2013; Schuetz et al., 2012). Indeed, it is unlikely that any single objective function could faithfully represent the possible spectrum of metabolic strategies across many different conditions. Future work could explore how COMETS predictions change upon implementing alternative condition-dependent objective functions. Such objective functions could be linear or quadratic (Segrè et al., 2002) and could include constraints associated with genetic regulation (Becker and Palsson, 2008; Collins et al., 2012).

Future elaborations of COMETS can be envisioned to incorporate additional aspects of microbial physiology that play an important role in microbial ecosystems, such as chemotaxis, quorum sensing, and antibiotic warfare. For example, chemotaxis could be modeled using nonisotropic diffusion, as a function of specific metabolite gradients. Toxins or antibiotics could be modeled as additional diffusible molecules that affect the death rate of specific organisms. The fact that COMETS performed so well despite lacking these important components is likely a consequence of our use of communities designed to strongly rely on metabolic-based interactions. At the same time, metabolism plays a fundamental role in many microbial systems, and it will be interesting to use COMETS as a null model to explore whether metabolic interactions are sufficient to explain ecosystem dynamics. Although no preliminary assumption needs to be made about which nutrients may mediate an interaction, COMETS can be extended to arbitrarily complex metabolic interdependencies. For example, as shown here, extending a consortium from two way to three way requires no additional assumptions or effort, other than modifying the initial conditions. Along the same line, COMETS can be extended to any number of species (including genetically modified strains), while increasing at most linearly in computational complexity.

The increasing flow of metagenomic sequencing data provides top-down observational insight into the taxonomic and

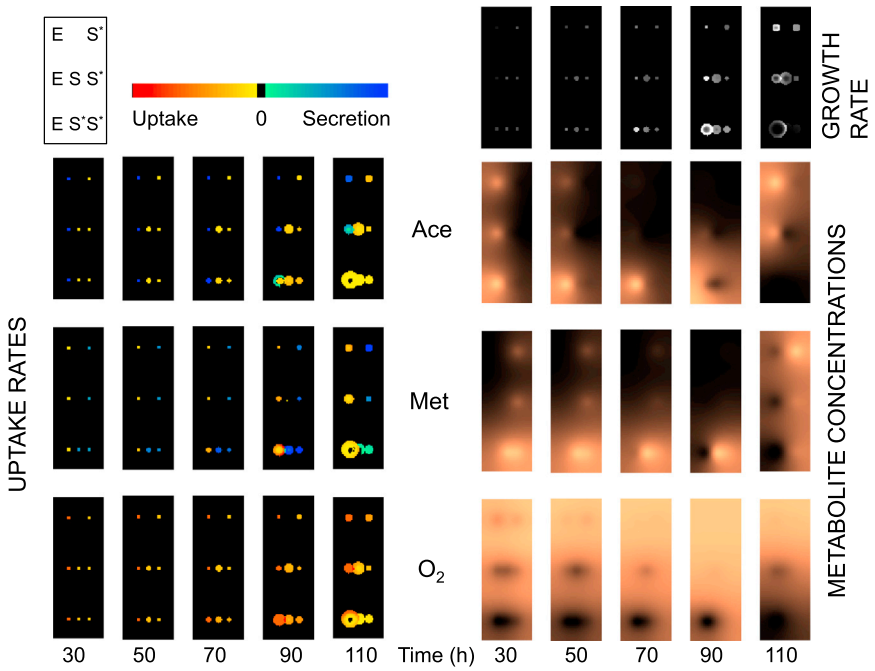

Figure 6. COMETS Predictions of Metabolites and Fluxes during the Metabolic Eclipse

Heatmaps of the spatial distributions of exchange fluxes (left side, 3 by 5 set of heatmaps), metabolite concentrations (right-side, copper-toned, 3 by 5 set of heatmaps) and growth rates (top-right, gray-shaded heatmaps) are shown at different time points during the "metabolic eclipse" simulation described in Figure 5. The legend in the top-left corner shows the relative positions of the simulated colonies, as in Figure 5A (E = *E. coli*; S = *S. enterica*). Fluxes (left) are scaled from excretion (blue) to uptake (red) for each lattice box at each of five time points for three key metabolites (acetate, methionine, and oxygen). Metabolite concentrations scale from low (dark) to high (bright). Fluxes are normalized across all time points; metabolites are normalized within each time point (to make early low concentration levels visible).

functional dynamics of microbial communities in different environments. Our work shows that there is a complementary, mechanistic, bottom-up way of studying how ecosystem dynamics may be ultimately understood in terms of its constituents' genomes. This approach is directly amenable to experimental testing and paves the way for new computationally driven directions in synthetic ecology. Despite the fact that our current work has been focused on small engineered communities, the concepts and algorithms we developed should be applicable and relevant to natural microbial consortia as well.

EXPERIMENTAL PROCEDURES

COMETS Variables

COMETS simulates the biomass and metabolite dynamics of multiple microbial species in physical space. Physical space (in 2D) is discretized into what could be thought of as an N by M grid of "boxes" whose location is defined by a pair of coordinates (x,y), with $x = 1,\ldots,N$ and $y = 1,\ldots,M$. Each box corresponds to a square of size L by L, where L is the minimal length scale, or the spatial resolution of COMETS (see Supplemental Experimental Procedures).

Each box can contain different microbial species and extracellular metabolites. Microbial species' abundances are described as the amounts of the corresponding biomass in each box. We denote with $B^{\alpha}_{(x,y)}$ the amount (in g dry cell weight) of biomass of species α present in a box at position (x,y), and with $Q^{m}_{(x,y)}$ the amount (in mmol) of metabolite m present in a box at position (x,y). Note that both biomass and metabolite abundances are time-dependent variables, i.e., $Q^{m}_{(x,y)} = Q^{m}_{(x,y)}(t)$ and $B^{\alpha}_{(x,y)} = B^{\alpha}_{(x,y)}(t)$. For each metabolite in each box, we can define a concentration $C^{m}_{(x,y)} = Q^{m}_{(x,y)}/V$ in mmol/ml.

Biomass in each box can increase due to cellular growth, or decrease due to microbial death. In addition, upon growth, biomass can expand from a given box to a neighboring one, a process that we currently model as slow diffusion. Metabolite levels in each box can change due to secretion or uptake by the microbial biomass present in the same box, or due to diffusion in/from neighboring boxes. The details of how biomass and metabolite levels change are described next.

COMETS Biomass Dynamics

The amount of biomass produced by a given population of microbes per unit time is estimated based on the nutrients available in the environment, and on the capacity of the organism's metabolism to transform such nutrients into biomass. Toward this goal, we employ a pseudodynamic version of FBA known as dynamic FBA, or dFBA (Mahadevan et al., 2002; Orth et al., 2010).

Following a standard notation, we call $\boldsymbol{S}^{\alpha}$ the stoichiometric matrix of a species α. Matrix element $\boldsymbol{S}^{\alpha}_{i,j}$ denotes the number of molecules of intracellular metabolite i that participate in reaction j (positive if metabolite i is a product, negative if it is a reactant). Each reaction is associated with a flux v^{α}_{j} (measured in mmol/(gDW*hr), giving rise to a vector $\boldsymbol{v}^{\alpha}$. The basic linear programming problem of FBA (for species α) can be written as follows:

$$\begin{aligned} &\text{Maximize} && \boldsymbol{Z}^{T}\boldsymbol{v}^{\alpha} \\ &\text{Subject to} && \boldsymbol{S}^{\alpha}\boldsymbol{v}^{\alpha} = 0 \\ & && LB^{\alpha}_{j} \le v^{\alpha}_{j} \le UB^{\alpha}_{j} \quad j = 1,\ldots,n \end{aligned} \qquad \text{Equation 1}$$

where $\boldsymbol{Z}$ defines the objective function, taken to be by default maximization of biomass production (see Discussion). The vectors $\boldsymbol{LB}^{\alpha}$ and $\boldsymbol{UB}^{\alpha}$ correspond to the lower and upper bounds to all fluxes respectively. As detailed below, the dynamic calculation of these bounds is an important aspect of COMETS.

In the dFBA formulation of COMETS, each step, for each species, consists of two main processes:

(1) Calculation of upper bounds for uptake rates. In line with previous FBA computations, exchange fluxes balance flow in and out of each model (see Orth et al., 2010 for additional discussion). What is unique to the dFBA formulation of COMETS is the implementation of additional environment-dependent constraints on these uptake/secretion fluxes. Upper bounds on uptake fluxes for the dFBA calculation are estimated based on a concentration-dependent saturating function, in analogy with Michaelis-Menten kinetics (Feng et al., 2012). Given an environmental concentration C^{m} of m (in a given box), the upper bound to u_m is given by the following saturation curve:

$$UB^{\alpha}_{m} = \frac{V^{\alpha,m}_{\max}[C_m]^{n}}{[C_m]^{n} + K^{\alpha,m}_{M}}, \qquad \text{Equation 2}$$

where n is a Hill coefficient (currently set to 1), $V^{\alpha,m}_{\max}$ is the maximal rate, and $K^{\alpha,m}_{M}$ is a binding constant.

(2) Solution of FBA problem and update of biomass and extracellular metabolite levels. Upon setting all upper bounds based on the

dynamically changing environmental concentrations, an FBA problem is solved for each species in each box, as described in Equation 1. Next, the abundances of biomass (for all species) and environmental metabolites are updated in each box, according to the following discrete update rules:

$$B^{\alpha}_{(x,y)}(t+\Delta t) = B^{\alpha}_{(x,y)}(t) + B^{\alpha}_{(x,y)}(t) \cdot v^{\alpha}_{growth} \cdot \Delta t$$

$$Q^{m}_{(x,y)}(t+\Delta t) = Q^{m}_{(x,y)}(t) + u^{\alpha}_{m} \cdot B^{\alpha}_{(x,y)}(t) \cdot \Delta t,$$

where v^{α}_{growth} is the growth rate of the corresponding species (in that specific box, [x,y]), and u^{α}_{m} is the rate of uptake/secretion of metabolite m by species α.

Thus, starting with a user-defined initial condition, a dFBA time step is performed on each box in the grid. Each box is updated independently. If there are multiple species present in a single box, they compete for media and space (i.e., a preset total carrying capacity per box). In this case, the order in which FBA is done is randomized among the species in each box.

In addition to biomass increase due to cellular growth, at each time cycle COMETS evaluates the extent of biomass reduction, due to dilution or cell death.

Diffusion

Diffusion steps are alternated with growth steps, predicting how biomass and extracellular metabolites propagate across the lattice. COMETS numerically computes approximate solutions to the standard two-dimensional diffusion equation on a 2D lattice, by using an alternating direction implicit (ADI) scheme with a central difference formulation (Peaceman and Rachford, 1955) as used in similar individual-based models (Chung et al., 2010; Gerlee and Anderson, 2008) (see Figure S1). This diffusion step is applied to biomass and media with substantially different diffusion coefficients. If the different species in the model are not allowed to exist in the same box (an option set by the user), then they undergo diffusion in random order; all boxes occupied by other species are treated as Neumann boundaries. Diffusion is applied separately to each medium component. Although metabolite-specific diffusion constants may be introduced if known, here we use the same value for all metabolites. Some boxes may represent physical barriers, which could be used to model different environmental topologies (e.g., Petri dish or a microfluidic device).

COMETS Download

COMETS executables, code, instructions, and examples can be downloaded at http://comets.bu.edu (see also Figure S2, related to Figure 1).

In Silico Experiments

We tested the predictive power of COMETS with metabolic models of *E. coli* (iJO_1366) (Orth et al., 2011), *S. enterica* (iRR_1083) (Raghunathan et al., 2009), and *M. extorquens* AM1 (Klitgord and Segrè, 2010). Standard FBA models were converted to COMETS format with the script provided on the COMETS website. Mutant *E. coli* and *M. extorquens* models were constructed by constraining flux through knocked out reactions to zero. A mutant *S. enterica* model was constructed that excreted methionine at a rate consistent with empirical observations. To achieve this, we added on the right side of the growth reaction 0.5 mmol/gDW of excreted extracellular methionine, balanced by an equal amount of intracellular methionine consumed (at the left side of the reaction equation). A Δ*hprA M. extorquens* model was constructed by constraining flux through the knocked out reaction to zero.

In silico environments were consistent with carbon limited minimal media (Table S1). Square lattices were constructed with individual boxes either 0.02 (Figure 2) or 0.05 cm a side (Figures 3, 4, 5, and 6). The amount of carbon under each box was calculated based on standard 25 ml plates (for example, 5 g/l glucose media was implemented as 0.0088 mmol/cm^2). Oxygen depletion has been observed inside colonies (Peters et al., 1987; Wimpenny and Coombs, 1983) so oxygen concentrations were constrained to 0.25 mmol/cm^2. Trace metals and other minor components of media were provided at a concentration of 1,000 mmol/box so that they were not limiting.

Simulations were executed with parameters based on published values (see also Table 1). Metabolite diffusion was set to 5×10^{-6} cm^2/s in agreement with sugar diffusion in Stewart (2003). Biomass diffusion was set to 3×10^{-9} cm^2/s for most simulations based on Korolev et al. (2011). The colony expansion simulations were run with a biomass diffusion of 3×10^{-10} cm^2/s because they were carried out on 1.5% agar plates rather than the 0.8% agarose used in all other experiments. Michaelis-Menten parameters were set to canonical values of K_m = 0.01 mM and V_{max} = 10 mmol g^{-1} hr^{-1} for all metabolites, well within the range of observed values (Gosset, 2005). An upper bound on biomass per box on the lattice was set based on the observation that *E. coli* colonies do not exceed a height of approximately 0.2 mm (Lewis and Wimpenny, 1981). Cell death rate was set to 1% per time step (Saint-Ruf et al., 2004). The time step for all simulations was 0.1 hr.

Strains Used Experimentally

The experimental data we collected involved strains of *E. coli* K-12, *S. enterica* LT2, and *M. extorquens* AM1. The *E. coli* was an isolate from the Keio collection (Δ*metB* CGSC# 10824, [Baba et al., 2006], erroneously referred to as Δ*metA* in Harcombe, 2010) with the *lac* operon replaced via conjugation with *E. coli HfrH PO1 relA1 thi-1 spoT supQ80 nad57*::Tn10. The methionine excreting *S. enterica* LT2 mutant was created through a combination of engineering and selection (Harcombe 2010). The Δ*hprA M. extorquens* was created previously (Marx, 2008).

Colony Expansion Comparisons

The *E. coli* colony growth dynamics were compared to results from Lewis and Wimpenny (1981). They made minimal media plates with 15 g/l bacto-agar and 0.5% (w/v) of glucose, lactate, or acetate. Plates were inoculated with a glass needle technique, incubated at 37°C, and measured microscopically. Average profiles were determined and used to calculate the radial growth rate. These data were compared against COMETS by simulating growth of a colony on each of the carbon sources. Colonies were initiated with 3×10^{-7} g biomass in the center of a 50 × 50 lattice with a box width of 0.02 cm. The diameter at various time points was based on the number of boxes with more than 10^{-7} g biomass/box along a horizontal line through the center of the colony.

Two-Species Consortium

The two-species ratio tests involved mixed cultures grown as a lawn on petri dishes or in simulations. Experimentally, *E. coli* and *S. enterica* were grown overnight in permissive media and then mixed at a ratio of 1:99 and 99:1. Five microliters of these mixtures was spread on 5 mm plates of lactose Hypho minimal media (2.92 mM lactose, 7.26 mM K_2HPO_4, 0.88 mM NaH_2PO_4, 1.89 mM $[NH_4]_2SO_4$, 0.41 mM $MgSO_4$, 1 ml of a metal mix based on Delaney et al., 2013 [recipe in Table S2]). The plates were allowed to grow for 2 days at 37°C. At the end of this time, colony-forming units (cfus) were determined by washing and scraping plates with 720 μl of minimal media and then spreading dilutions on LB plates. On LB, both *E. coli* and *S. enterica* can grow independently, and X-gal (5-bromo-4-chloro-3-indolyl-β-D-galactopyranoside) was included in the plates so that blue *E. coli* colonies could be distinguished from white *S. enterica* colonies. Comparison to COMETS was carried out by randomly distributing 100 boxes in the relevant species ratios each with 3×10^{-7} biomass across a 25 × 25 lattice (individual box width = 0.05 cm). Cell overlap was allowed and the total biomass of each type was determined after 48 hr of simulated growth. Three replicate simulations were carried out for each treatment.

The impact of space and orientation on the consortium involved detailed placement of cells. Wet lab experiments were carried out with overnight cultures of *E. coli* and *S. enterica* that were washed and concentrated to ~10^9 cells/ml. Cells were added to wells in a 384-well plate in the desired layout. A 384-pin head was then used to stamp the cells onto a petri dish so that *E. coli* was inoculated 10 mm from distal *S. enterica*, and when relevant intermediate *S. enterica* was exactly halfway between. Different treatments were separated by 30 mm. These plates were grown at 37°C with high humidity for 10 days. The biomass produced in the eclipse experiment was assayed by cutting colonies out of the plate, breaking up the agar, vortexing extensively, plating on permissive LB plates, and counting colonies. COMETS

Please cite this article in press as: Harcombe et al., Metabolic Resource Allocation in Individual Microbes Determines Ecosystem Interactions and Spatial Dynamics, Cell Reports (2014), http://dx.doi.org/10.1016/j.celrep.2014.03.070

comparisons were carried out in a 50 × 140 lattice of 0.05 cm boxes. Boxes were inoculated with 2×10^{-6} g of biomass at the appropriate distances.

Three-Species Consortium

Experiments with the three-species consortium involved very similar protocols to those with the two-species consortium. Each species was grown in permissive media, and then the species were combined volumetrically at ratios of 1:100:100 or 100:1:100 *E. coli:S. enterica:M. extorquens*. Ten microliters of one of the mixtures was added to each of three replicate methylamine-lactose minimal medium plates ($[NH_4]_2SO_4$ replaced with 1.9 mM Na_2SO_4, and 2.51 mM methylamine × HCl added). After 96 hr incubation, the surface of the plates was scrubbed with 720 μl of minimal media. An aliquot of 5 μl of the resultant suspension was then transferred to a fresh plate, spread, and incubated for 96 hr. A total of five transfers were completed, and at each transfer the ratios of the three species were determined from their cfu concentrations.

This process was emulated in COMETS by randomly distributing 100 boxes in the relevant species ratios each with 3×10^{-7} biomass across a 15 × 15 lattice (individual box width = 0.05 cm). The initial ratios based on cfu data were 1:8:92 and 16:1:83 *E. coli:S. enterica:M. extorquens*. The simulations were carried out for 96 hr at which point the species ratios were calculated. A new lattice was then randomly populated with the initial amount of biomass in the new ratios to mimic the laboratory transfer regimen. Three replicate simulations were carried out for each of the treatments.

SUPPLEMENTAL INFORMATION

Supplemental Information includes Supplemental Experimental Procedures, six figures, and two tables and can be found with this article online at http://dx.doi.org/10.1016/j.celrep.2014.03.070.

AUTHOR CONTRIBUTIONS

D.S., C.J.M., W.R.H., and W.J.R. designed the study and wrote the manuscript; W.J.R. and I.D. wrote the COMETS code; W.R.H. implemented the engineered ecosystem simulations and experiments; A.B. contributed to the experiments; B.R.G., A.H.L., G.B., A.K., N.L., and P.M. contributed specific portions of the computational analysis; and D.S. coordinated the project.

ACKNOWLEDGMENTS

This work was supported by the Office of Science (BER), U.S. Department of Energy (grant DE-SC0004962 to D.S.). D.S., W.J.R., I.D., B.R.G., and A.K. were supported also by the NASA Astrobiology Institute (NNA08CN84A) and NIH (5R01GM089978 and 5R01GM103502-06). G.B. was supported by IGERT NSF DGE-0654108. W.R.H. was supported also by NIH NRSA 1F32GM090760 and DOE award to C.J.M. (DE-SC0006731). N.L. was supported by NSF GRFP DGE-1247312. P.M. was partially supported by NIH K25 GM086909. A.H.L. was supported by NSF DGE-0741448. The authors are grateful for useful conversations with Niels Klitgord, Melanie Muller, and with members of the Segrè and Marx labs.

Received: August 14, 2013
Revised: February 1, 2014
Accepted: March 28, 2014
Published: May 1, 2014

REFERENCES

Baba, T., Ara, T., Hasegawa, M., Takai, Y., Okumura, Y., Baba, M., Datsenko, K.A., Tomita, M., Wanner, B.L., and Mori, H. (2006). Construction of Escherichia coli K-12 in-frame, single-gene knockout mutants: the Keio collection. Mol. Syst. Biol *2*, 2006.0008.

Balagaddé, F.K., Song, H., Ozaki, J., Collins, C.H., Barnet, M., Arnold, F.H., Quake, S.R., and You, L. (2008). A synthetic *Escherichia coli* predator-prey ecosystem. Mol. Syst. Biol. *4*, 187.

Becker, S.A., and Palsson, B.O. (2008). Context-specific metabolic networks are consistent with experiments. PLoS Comput. Biol. *4*, e1000082.

Ben-Jacob, E., Cohen, I., and Gutnick, D.L. (1998). Cooperative organization of bacterial colonies: from genotype to morphotype. Annu. Rev. Microbiol. *52*, 779–806.

Berg, H.C., and Purcell, E.M. (1977). Physics of chemoreception. Biophys. J. *20*, 193–219.

Bordel, S., Agren, R., and Nielsen, J. (2010). Sampling the solution space in genome-scale metabolic networks reveals transcriptional regulation in key enzymes. PLoS Comput. Biol. *6*, e1000859.

Bull, J.J., and Harcombe, W.R. (2009). Population dynamics constrain the cooperative evolution of cross-feeding. PLoS ONE *4*, e4115.

Chistoserdova, L., Kalyuzhnaya, M.G., and Lidstrom, M.E. (2009). The expanding world of methylotrophic metabolism. Annu. Rev. Microbiol. *63*, 477–499.

Chung, C.A., Lin, T.-H., Chen, S.-D., and Huang, H.-I. (2010). Hybrid cellular automaton modeling of nutrient modulated cell growth in tissue engineering constructs. J. Theor. Biol. *262*, 267–278.

Collins, S.B., Reznik, E., and Segrè, D. (2012). Temporal expression-based analysis of metabolism. PLoS Comput. Biol. *8*, e1002781.

Cooper, A.L., Dean, A.C., and Hinshelwood, C. (1968). Factors affecting the growth of bacterial colonies on agar plates. Proc. R. Soc. Lond. B Biol. Sci. *171*, 175–199.

Curtis, T.P., Sloan, W.T., and Scannell, J.W. (2002). Estimating prokaryotic diversity and its limits. Proc. Natl. Acad. Sci. USA *99*, 10494–10499.

De Martino, D., Figliuzzi, M., De Martino, A., and Marinari, E. (2012). A scalable algorithm to explore the Gibbs energy landscape of genome-scale metabolic networks. PLoS Comput. Biol. *8*, e1002562.

Delaney, N.F., Kaczmarek, M.E., Ward, L.M., Swanson, P.K., Lee, M.-C., and Marx, C.J. (2013). Development of an optimized medium, strain and high-throughput culturing methods for *Methylobacterium extorquens*. PLoS ONE *8*, e62957.

Denef, V.J., Mueller, R.S., and Banfield, J.F. (2010). AMD biofilms: using model communities to study microbial evolution and ecological complexity in nature. ISME J. *4*, 599–610.

Dethlefsen, L., McFall-Ngai, M., and Relman, D.A. (2007). An ecological and evolutionary perspective on human-microbe mutualism and disease. Nature *449*, 811–818.

Estrela, S., and Brown, S.P. (2013). Metabolic and demographic feedbacks shape the emergent spatial structure and function of microbial communities. PLoS Comput. Biol. *9*, e1003398.

Falkowski, P.G., Fenchel, T., and Delong, E.F. (2008). The microbial engines that drive Earth's biogeochemical cycles. Science *320*, 1034–1039.

Feng, X., Xu, Y., Chen, Y., and Tang, Y.J. (2012). Integrating flux balance analysis into kinetic models to decipher the dynamic metabolism of *Shewanella oneidensis* MR-1. PLoS Comput. Biol. *8*, e1002376.

Fleming, R.M.T., Maes, C.M., Saunders, M.A., Ye, Y., and Palsson, B.Ø. (2012). A variational principle for computing nonequilibrium fluxes and potentials in genome-scale biochemical networks. J. Theor. Biol. *7*, 71–77.

Freilich, S., Zarecki, R., Eilam, O., Segal, E.S., Henry, C.S., Kupiec, M., Gophna, U., Sharan, R., and Ruppin, E. (2011). Competitive and cooperative metabolic interactions in bacterial communities. Nat. Commun. *2*, 589.

Gerlee, P., and Anderson, A.R. (2008). A hybrid cellular automaton model of clonal evolution in cancer: the emergence of the glycolytic phenotype. J. Theor. Biol. *250*, 705–722.

Gosset, G. (2005). Improvement of *Escherichia coli* production strains by modification of the phosphoenolpyruvate:sugar phosphotransferase system. Microb. Cell Fact. *4*, 14.

Gudelj, I., Weitz, J.S., Ferenci, T., Claire Horner-Devine, M., Marx, C.J., Meyer, J.R., and Forde, S.E. (2010). An integrative approach to understanding microbial diversity: from intracellular mechanisms to community structure. Ecol. Lett. *13*, 1073–1084.

Harcombe, W. (2010). Novel cooperation experimentally evolved between species. Evolution *64*, 2166–2172.

Harcombe, W.R., Delaney, N.F., Leiby, N., Klitgord, N., and Marx, C.J. (2013). The ability of flux balance analysis to predict evolution of central metabolism scales with the initial distance to the optimum. PLoS Comput. Biol. *9*, e1003091.

Henry, C.S., DeJongh, M., Best, A.A., Frybarger, P.M., Linsay, B., and Stevens, R.L. (2010). High-throughput generation, optimization and analysis of genome-scale metabolic models. Nat. Biotechnol. *28*, 977–982.

Hernández-Sánchez, V., Lang, E., and Wittich, R.-M. (2013). The Three-Species Consortium of Genetically Improved Strains *Cupriavidus necator* RW112, *Burkholderia xenovorans* RW118, and *Pseudomonas pseudoalcaligenes* RW120 Grows with Technical Polychlorobiphenyl, Aroclor 1242. Front. Microbiol. *4*, 90.

Hillesland, K.L., and Stahl, D.A. (2010). Rapid evolution of stability and productivity at the origin of a microbial mutualism. Proc. Natl. Acad. Sci. USA *107*, 2124–2129.

Kamath, R.S., and Bungay, H.R. (1988). Growth of yeast colonies on solid media. J. Gen. Microbiol. *134*, 3061–3069.

Kerner, A., Park, J., Williams, A., and Lin, X.N. (2012). A programmable *Escherichia coli* consortium via tunable symbiosis. PLoS ONE *7*, e34032.

Kerr, B., Riley, M.A., Feldman, M.W., and Bohannan, B.J. (2002). Local dispersal promotes biodiversity in a real-life game of rock-paper-scissors. Nature *418*, 171–174.

Khandelwal, R.A., Olivier, B.G., Röling, W.F.M., Teusink, B., and Bruggeman, F.J. (2013). Community flux balance analysis for microbial consortia at balanced growth. PLoS ONE *8*, e64567.

Kim, H.J., Boedicker, J.Q., Choi, J.W., and Ismagilov, R.F. (2008). Defined spatial structure stabilizes a synthetic multispecies bacterial community. Proc. Natl. Acad. Sci. USA *105*, 18188–18193.

Klitgord, N., and Segrè, D. (2010). Environments that induce synthetic microbial ecosystems. PLoS Comput. Biol. *6*, e1001002.

Klitgord, N., and Segrè, D. (2011). Ecosystems biology of microbial metabolism. Curr. Opin. Biotechnol. *22*, 541–546.

Korolev, K.S., Xavier, J.B., Nelson, D.R., and Foster, K.R. (2011). A quantitative test of population genetics using spatiogenetic patterns in bacterial colonies. Am. Nat. *178*, 538–552.

Kreft, J.U., Booth, G., and Wimpenny, J.W. (1998). BacSim, a simulator for individual-based modelling of bacterial colony growth. Microbiology *144*, 3275–3287.

Kreft, J.U., Picioreanu, C., Wimpenny, J.W., and van Loosdrecht, M.C. (2001). Individual-based modelling of biofilms. Microbiology *147*, 2897–2912.

Lewis, M.W., and Wimpenny, J.W. (1981). The influence of nutrition and temperature on the growth of colonies of *Escherichia coli* K12. Can. J. Microbiol. *27*, 679–684.

Louie, K.B., Bowen, B.P., McAlhany, S., Huang, Y., Price, J.C., Mao, J.H., Hellerstein, M., and Northen, T.R. (2013). Mass spectrometry imaging for in situ kinetic histochemistry. Sci. Rep. *3*, 1656.

Lozupone, C.A., Stombaugh, J.I., Gordon, J.I., Jansson, J.K., and Knight, R. (2012). Diversity, stability and resilience of the human gut microbiota. Nature *489*, 220–230.

MacLean, R.C., and Gudelj, I. (2006). Resource competition and social conflict in experimental populations of yeast. Nature *441*, 498–501.

Mahadevan, R., Edwards, J.S., and Doyle, F.J., 3rd. (2002). Dynamic flux balance analysis of diauxic growth in *Escherichia coli*. Biophys. J. *83*, 1331–1340.

Marx, C.J. (2008). Development of a broad-host-range sacB-based vector for unmarked allelic exchange. BMC Res. Notes *1*, 1.

May, R.M. (1973). Stability and complexity in model ecosystems. Monogr. Popul. Biol. *6*, 1–235.

McCloskey, D., Palsson, B.Ø., and Feist, A.M. (2013). Basic and applied uses of genome-scale metabolic network reconstructions of *Escherichia coli*. Mol. Syst. Biol. *9*, 661.

Miller, L.D., Mosher, J.J., Venkateswaran, A., Yang, Z.K., Palumbo, A.V., Phelps, T.J., Podar, M., Schadt, C.W., and Keller, M. (2010). Establishment and metabolic analysis of a model microbial community for understanding trophic and electron accepting interactions of subsurface anaerobic environments. BMC Microbiol. *10*, 149.

Mougi, A., and Kondoh, M. (2012). Diversity of interaction types and ecological community stability. Science *337*, 349–351.

Orth, J.D., Thiele, I., and Palsson, B.Ø. (2010). What is flux balance analysis? Nat. Biotechnol. *28*, 245–248.

Orth, J.D., Conrad, T.M., Na, J., Lerman, J.A., Nam, H., Feist, A.M., and Palsson, B.Ø. (2011). A comprehensive genome-scale reconstruction of Escherichia coli metabolism—2011. Mol. Syst. Biol. *7*, 535.

Palumbo, S.A., Johnson, M.G., Rieck, V.T., and Witter, L.D. (1971). Growth measurements on surface colonies of bacteria. J. Gen. Microbiol. *66*, 137–143.

Park, J., Kerner, A., Burns, M.A., and Lin, X.N. (2011). Microdroplet-enabled highly parallel co-cultivation of microbial communities. PLoS ONE *6*, e17019.

Peaceman, D.W., and Rachford, H.H., Jr. (1955). The Numerical Solution of Parabolic and Elliptic Differential Equations. J. Soc. Ind. Appl. Math. *3*, 28–41.

Peters, A.C., Wimpenny, J.W., and Coombs, J.P. (1987). Oxygen profiles in, and in the agar beneath, colonies of *Bacillus cereus, Staphylococcus albus* and *Escherichia coli*. J. Gen. Microbiol. *133*, 1257–1263.

Pfeiffer, T., and Bonhoeffer, S. (2003). An evolutionary scenario for the transition to undifferentiated multicellularity. Proc. Natl. Acad. Sci. USA *100*, 1095–1098.

Pipe, L.Z., and Grimson, M.J. (2008). Spatial-temporal modelling of bacterial colony growth on solid media. Mol. Biosyst. *4*, 192–198.

Pirt, S.J. (1967). A kinetic study of the mode of growth of surface colonies of bacteria and fungi. J. Gen. Microbiol. *47*, 181–197.

Raghunathan, A., Reed, J., Shin, S., Palsson, B., and Daefler, S. (2009). Constraint-based analysis of metabolic capacity of *Salmonella typhimurium* during host-pathogen interaction. BMC Syst. Biol. *3*, 38.

Ramette, A., and Tiedje, J.M. (2007). Multiscale responses of microbial life to spatial distance and environmental heterogeneity in a patchy ecosystem. Proc. Natl. Acad. Sci. USA *104*, 2761–2766.

Reznik, E., Mehta, P., and Segrè, D. (2013). Flux imbalance analysis and the sensitivity of cellular growth to changes in metabolite pools. PLoS Comput. Biol. *9*, e1003195.

Rieck, V.T., Palumbo, S.A., and Witter, L.D. (1973). Glucose availability and the growth rate of colonies of *Pseudomonas fluorescens*. J. Gen. Microbiol. *74*, 1–8.

Sachs, J.L., Mueller, U.G., Wilcox, T.P., and Bull, J.J. (2004). The evolution of cooperation. Q. Rev. Biol. *79*, 135–160.

Saint-Ruf, C., Taddei, F., and Matic, I. (2004). Stress and survival of aging *Escherichia coli* rpoS colonies. Genetics *168*, 541–546.

Salimi, F., Zhuang, K., and Mahadevan, R. (2010). Genome-scale metabolic modeling of a clostridial co-culture for consolidated bioprocessing. Biotechnol. J. *5*, 726–738.

Scheibe, T.D., Mahadevan, R., Fang, Y., Garg, S., Long, P.E., and Lovley, D.R. (2009). Coupling a genome-scale metabolic model with a reactive transport model to describe in situ uranium bioremediation. Microb. Biotechnol. *2*, 274–286.

Schuetz, R., Zamboni, N., Zampieri, M., Heinemann, M., and Sauer, U. (2012). Multidimensional optimality of microbial metabolism. Science *336*, 601–604.

Segrè, D., Vitkup, D., and Church, G.M. (2002). Analysis of optimality in natural and perturbed metabolic networks. Proc. Natl. Acad. Sci. USA *99*, 15112–15117.

Shou, W., Ram, S., and Vilar, J.M.G. (2007). Synthetic cooperation in engineered yeast populations. Proc. Natl. Acad. Sci. USA *104*, 1877–1882.

Stewart, P.S. (2003). Diffusion in biofilms. J. Bacteriol. *185*, 1485–1491.

Stolyar, S., Van Dien, S., Hillesland, K.L., Pinel, N., Lie, T.J., Leigh, J.A., and Stahl, D.A. (2007). Metabolic modeling of a mutualistic microbial community. Mol. Syst. Biol. *3*, 92.

Please cite this article in press as: Harcombe et al., Metabolic Resource Allocation in Individual Microbes Determines Ecosystem Interactions and Spatial Dynamics, Cell Reports (2014), http://dx.doi.org/10.1016/j.celrep.2014.03.070

Turnbaugh, P.J., Ley, R.E., Hamady, M., Fraser-Liggett, C.M., Knight, R., and Gordon, J.I. (2007). The human microbiome project. Nature *449*, 804–810.

Vuilleumier, S., Chistoserdova, L., Lee, M.-C., Bringel, F., Lajus, A., Zhou, Y., Gourion, B., Barbe, V., Chang, J., Cruveiller, S., et al. (2009). *Methylobacterium* genome sequences: a reference blueprint to investigate microbial metabolism of C1 compounds from natural and industrial sources. PLoS ONE *4*, e5584.

Watrous, J.D., and Dorrestein, P.C. (2011). Imaging mass spectrometry in microbiology. Nat. Rev. Microbiol. *9*, 683–694.

Wimpenny, J.W. (1979). The growth and form of bacterial colonies. J. Gen. Microbiol. *114*, 483–486.

Wimpenny, J.W., and Coombs, J.P. (1983). Penetration of oxygen into bacterial colonies. J. Gen. Microbiol. *129*, 1239–1242.

Wintermute, E.H., and Silver, P.A. (2010). Emergent cooperation in microbial metabolism. Mol. Syst. Biol. *6*, 407.

Xavier, J.B., and Foster, K.R. (2007). Cooperation and conflict in microbial biofilms. Proc. Natl. Acad. Sci. USA *104*, 876–881.

Xavier, J.B., Picioreanu, C., and van Loosdrecht, M.C.M. (2005). A framework for multidimensional modelling of activity and structure of multispecies biofilms. Environ. Microbiol. *7*, 1085–1103.

Zomorrodi, A.R., and Maranas, C.D. (2012). OptCom: a multi-level optimization framework for the metabolic modeling and analysis of microbial communities. PLoS Comput. Biol. *8*, e1002363.

Cell Reports, Volume *7*

Supplemental Information

Metabolic Resource Allocation in Individual Microbes Determines Ecosystem Interactions and Spatial Dynamics

William R. Harcombe, William J. Riehl, Ilija Dukovski, Brian R. Granger, Alex Betts, Alex H. Lang, Gracia Bonilla, Amrita Kar, Nicholas Leiby, Pankaj Mehta, Christopher J. Marx, and Daniel Segrè

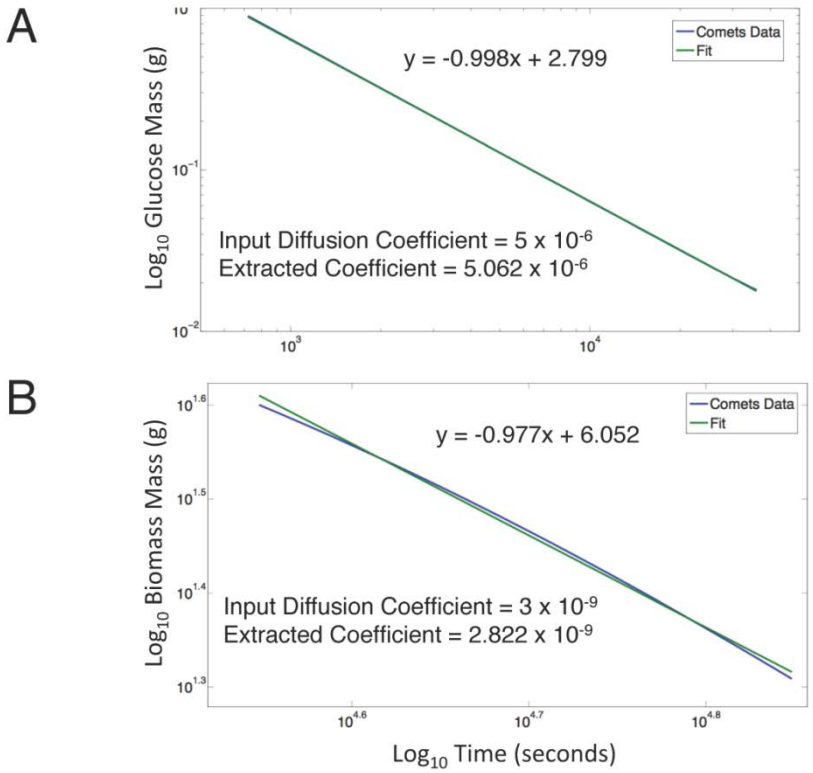

Figure S1 – Diffusion tests for glucose and biomass. The expected change in concentration over time is governed by

$$\Phi(r,t) = \frac{1}{4\pi Dt} e^{-r^2/4Dt}$$

where D is the desired diffusion coefficient, r is the radius of area with diffusing compound, and t is time. On a log-log (base 10) plot a straight line is expected with a slope of -1. Furthermore, a simulated diffusion coefficient can be calculated from

$$D = \frac{10^{-b}}{4\pi}(\Delta x)^2$$

and compared against the diffusion coefficient that was provided. Figure S1A shows glucose diffusion over 50 time steps from 0.2 to 10 hrs. The extracted slope has 0.2% error while the extracted diffusion coefficient has 1.2% error. Figure S1B shows biomass flow diffusion over 50 times steps from 10 hrs to 20 hrs. Since the biomass flow has a diffusion coefficient three orders of magnitude smaller, the delta function approximation breaks down for the same mass at a shorter time scale. However, on the longer time scale, the slope was within 2.4% and the diffusion coefficient was correct to 5.9%. For all subfigures, the initial condition was one pixel of 100g on a 100x100 grid of 0.2 cm^2 and a flux balance time step of 0.2 hours with 10 diffusion steps per flux balance time step.

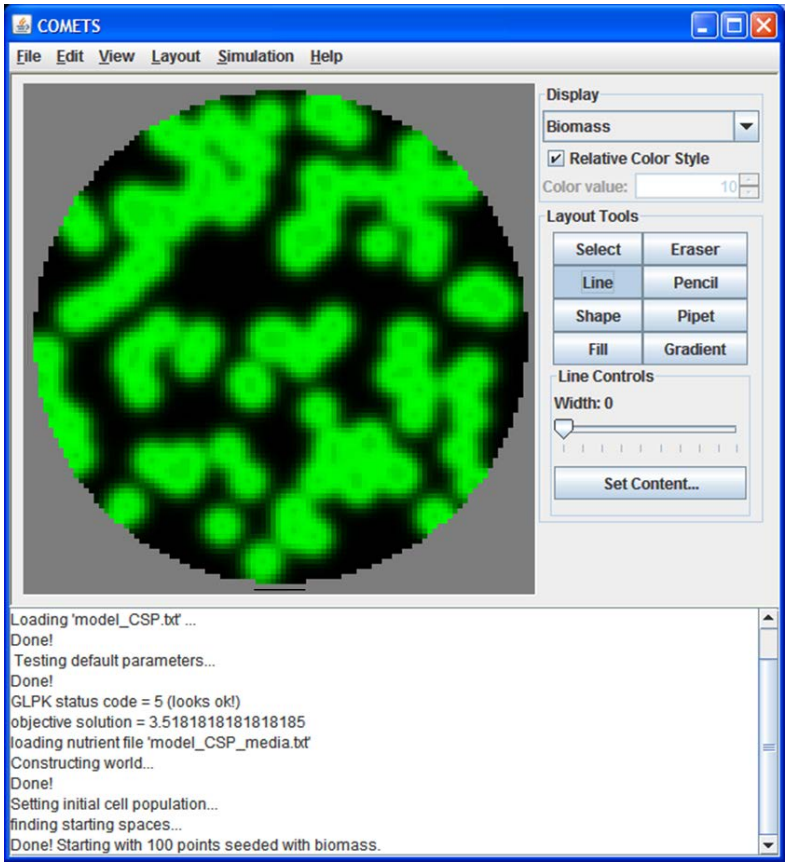

Figure S2 – A snapshot of the main graphic user interface of COMETS. In addition to visualizing the current spatial distribution of any species or metabolites, this interface makes it possible to upload, save or set initial conditions for *in silico* experiments. The initial conditions (abundance of organisms or metabolites) can be initialized at any individual discrete point in space, either using appropriate text files (see http://www.bu.edu/segrelab/comets/), or a phostoshop-like set of tools. Using these tools the user can literally "paint" the initial amounts of biomass for different species on the screen, as if this was a virtual Petri dish.

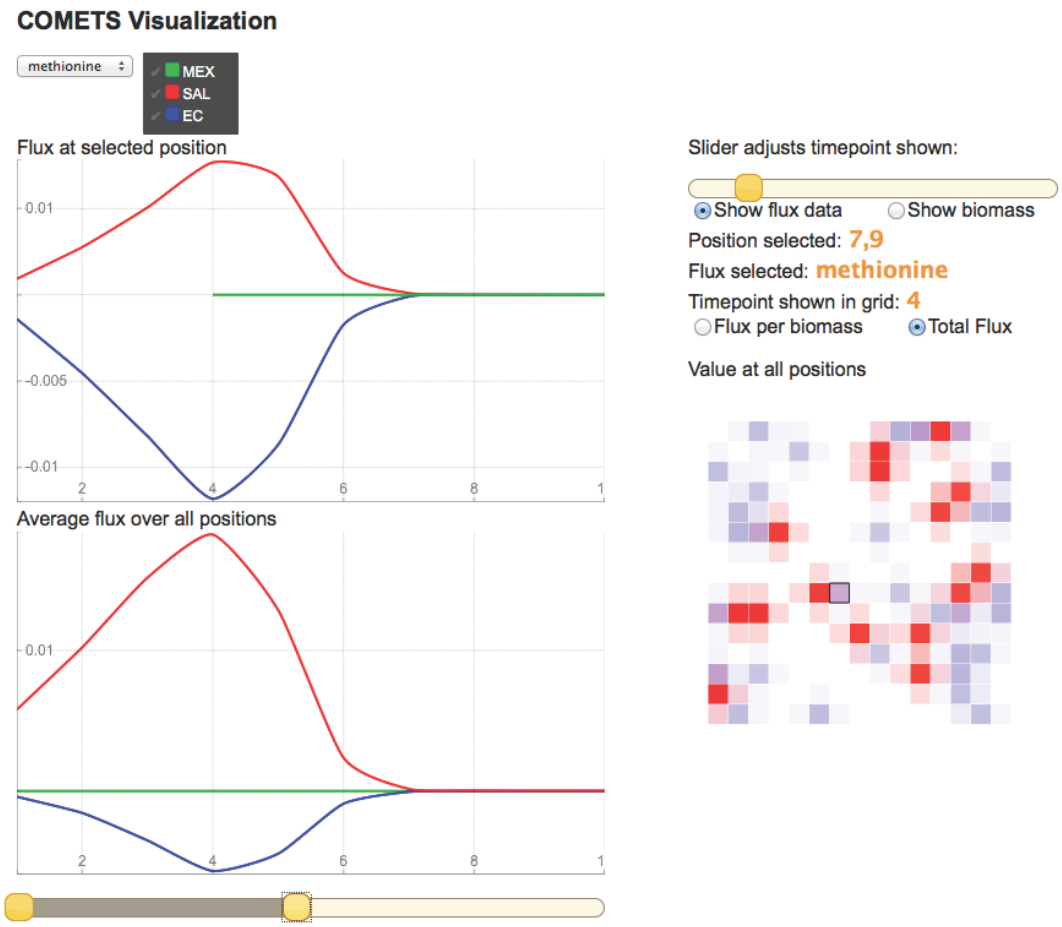

Figure S3 – The output data of a COMETS simulation can be very large, as it includes multiple variables (amount of biomass and complete flux vectors for different species, extracellular metabolite concentrations) for every discrete point in time and space. Thus, we have developed a set of scripts that allow users to explore this data in an efficient way, through an html-based visualization interface. The example shown here pertains to one of the simulations performed for the 3-species consortium. The corresponding interactive tool can be accessed at http://comets.bu.edu/viewer/.

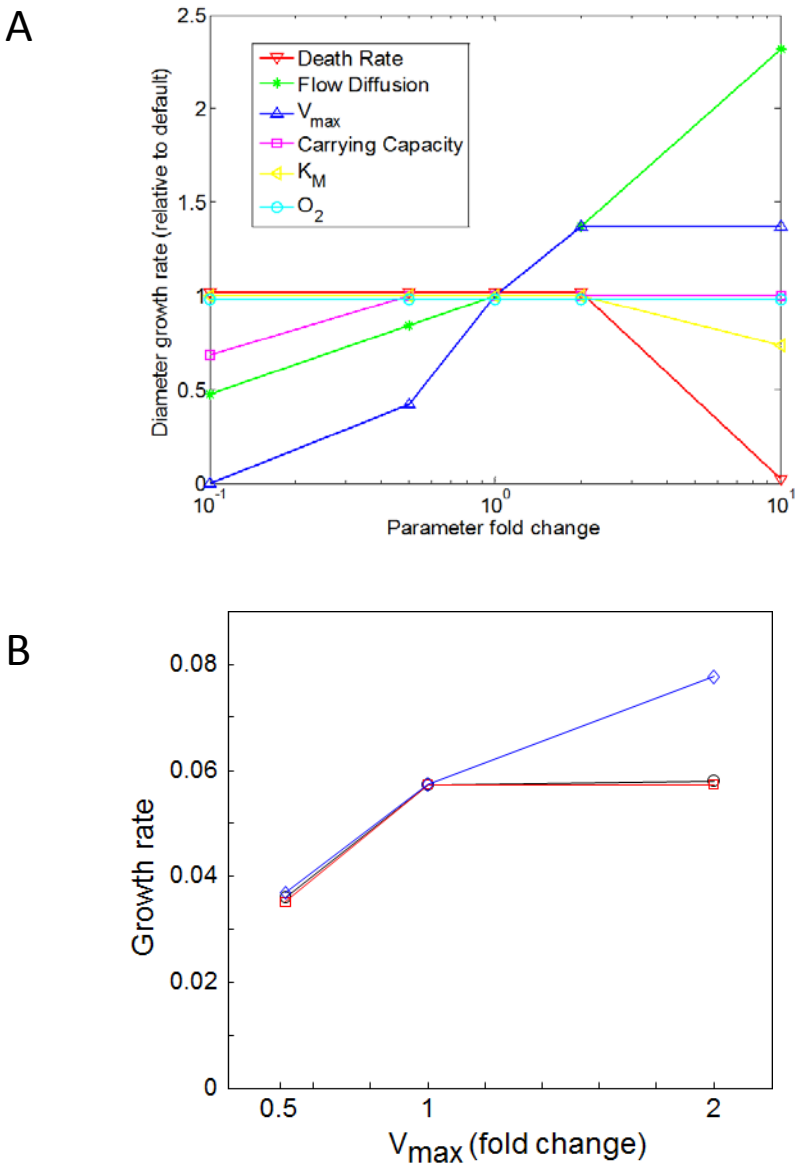

Figure S4 – Parameter sensitivity for the rate of *E. coli* colony expansion on glucose. **A** Lines connect the predicted rate of colony expansion as each parameter was individually multiplied by the listed perturbation factor. Unperturbed parameters were maintained at the values listed in Table 1. Changes of 2-fold had little impact on results across parameters. A 10-fold increase in diffusion led to less than a 2.5-fold change in rate of colony expansion. Colonies did not expand if V_{max} was dropped to 1 (while K_m remained at 0.01), or if death rate was increased to 10%. **B** Sensitivity of the initial growth rate of the total biomass as a function of the exchange parameter V_{max} for glucose (black), nitrogen (red) and oxygen (blue) uptake. The growth rates were calculated as the slope of the semilog plot of the total biomass vs. time. The figure indicates that the values of V_{max} for glucose and nitrogen are at their maximums beyond which the model is insensitive to their change. This is not the case for oxygen.

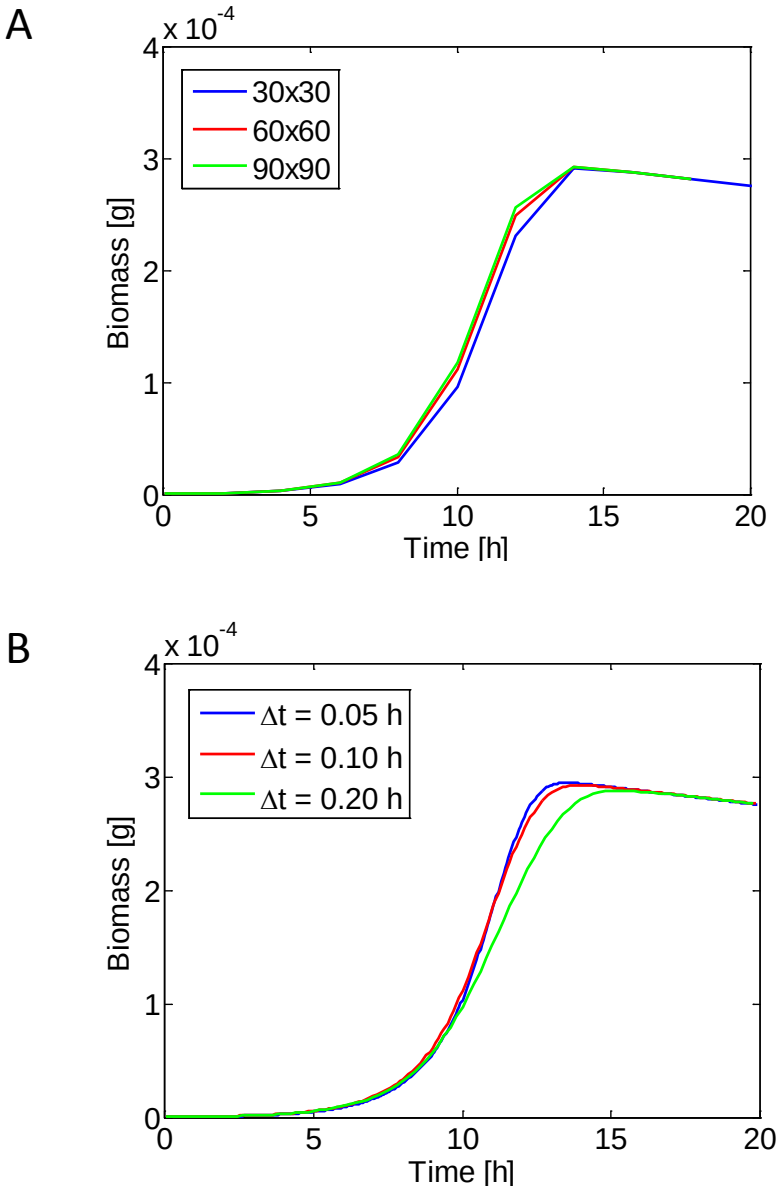

Figure S5 – Sensitivity of COMETS to spatial and time scales. **A** The total biomass growth curves display minor changes for increasing size of the finite spatial grid, and scale monotonically. The linear size of the simulation square was 0.6 cm in all three cases shown here. The growth curves correspond to simulations with the spatial area divided into grid of 30 by 30(blue), 60 by 60(red) and 90 by 90(green) squares, each with uniform biomass. The figure indicates that the difference between the curves becomes smaller with increasing grid size and would converge for an infinitely fine grid. **B** The total biomass growth curves display minor changes for decreasing finite simulation time step, and scale monotonically. The total simulation time was 20 hours. The growth curves correspond to simulations with discrete unit time step of 0.05 hours (blue), 0.1 hours (red) and 0.2 hours (green). The figure indicates that the difference between the growth curves becomes smaller with decreasing unit time step and would converge for an infinitesimally small time step.

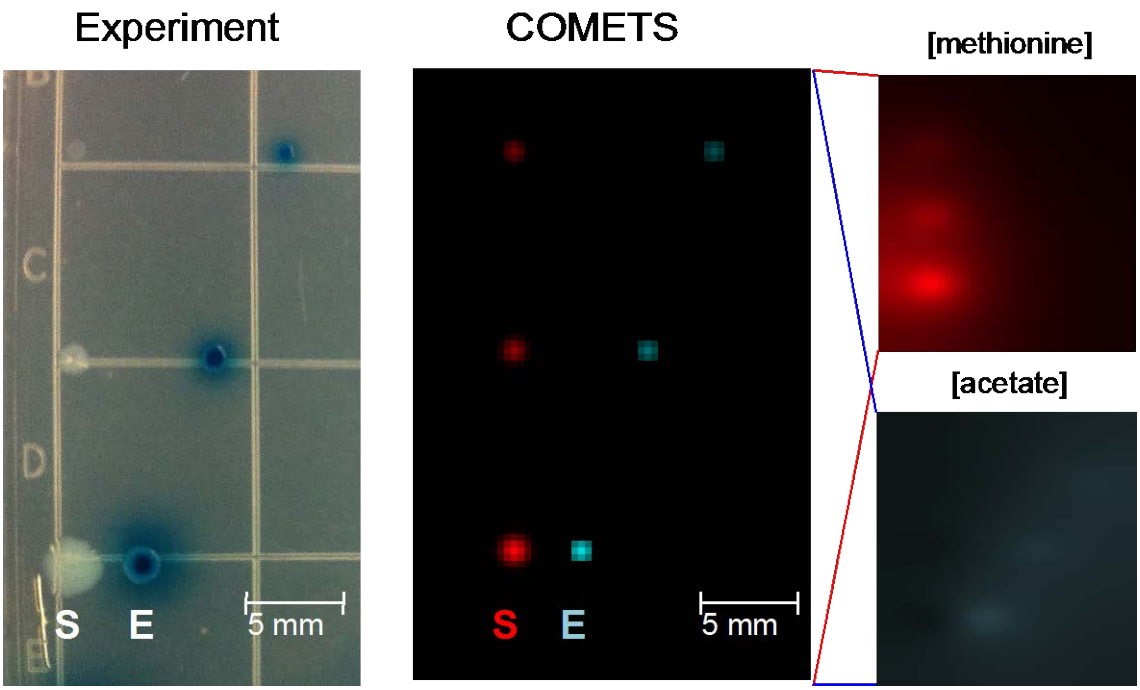

Figure S6 - Comparison of predictions and experimental results for the growth impact of increasing distance between mutualistic *S. enterica* (white colonies observed, red colonies predicted), and *E. coli* (blue colonies observed, and predicted – the blue on observed plates is the result of X-gal). Predicted metabolite gradients are displayed as insets for methionine (red) and acetate (blue).

Table S1 – Metabolite concentrations used to simulate minimal medium in COMETS. Lactose (lcts) was replaced with alternative carbon sources for individual *E. coli* colony simulations (glc = 3.5e-6, lac-L = 7.1e-6, or ac = 1.1e-5). Oxygen was lowered to maintain the same concentration with smaller pixel size (i.e. if box length (L)= 0.2 mm then o2 = 1e-5). For the 3-species consortium methylamine was added (mea = 2.0e-6).

Compound	mM per box
ca2[e]	1000.0
cl[e]	1000.0
cobalt2[e]	1000.0
cu2[e]	1000.0
fe2[e]	1000.0
fe3[e]	1000.0
k[e]	1000.0
lcts[e]	1.2e-5
mg2[e]	1000.0
mn2[e]	1000.0
mobd[e]	1000.0
nh4[e]	1000.0
ni2[e]	1000.0
o2[e]	6.2e-5
pi[e]	1000.0
so4[e]	1000.0
zn2[e]	1000.0

Table S2 - Metal Mix used in Hypho minimal media for lab experiments

Metal	1000x concentration (mM)
$ZnSO_4$	0.60
$CaCl_2$	9.98
$MnCl_2$	0.51
$(NH_4)_6Mo_7O_{24}$	1.00
$CuSO_4$	0.50
$CoCl_2$	1.00
Na_2WO_4	0.17
$FeSO_4$	8.88

Supplemental Experimental Procedures

Time scales

COMETS exploits a natural separation of time scales between growth and the diffusion of small molecules to efficiently model the complex dynamics in a computationally tractable manner that is physically consistent. The typical time scale associated with growth, t_{growth}, is set by cell doubling times and is of order 10^3-10^4 seconds. Importantly, the time step for simulating the diffusion of small molecules, t_D ~10 seconds, is chosen to be two to three orders of magnitude smaller than the doubling time. The diffusion time scale, $t_{D,}$ can be thought of as the time it takes a small molecule to diffuse one lattice spacing. For this reason, fixing t_D associates a length scale l with each point in our lattice. This length scale is related to the diffusion constant, D, of small metabolites and is given by $l^2 \sim Dt_D$. For small metabolites, $D \sim 10^{-5}$ cm^2/s, implying that we have a spatial resolution of about 10^{-2} cm per grid point.

COMETS performance

A COMETS simulation of a 100 by 100 grid, partially filled with biomass from a single species requires solving of the order of 1000 FBA problems per time cycle. Considering a time step of 0.1 h, COMETS performs approximately a 10^4 FBA cycles for 1h of real time simulation. On 32 CPUs (using a multi-thread version of COMETS), this will take approximately a minute.